ADR Shape Descriptor – Distance between Shape Centroids versus Shape Diameter

Reinhard Klette[a], Joviša Žunić[b]

[a] *The Department of Computer Science, The University of Auckland Auckland 1142, New Zealand*
[b] *Department of Computer Science, University of Exeter Exeter EX4 4QF, U.K.*
Also with the Mathematical Institute, Serbian Academy of Arts and Sciences, Belgrade

Abstract

In this paper we study the ADR shape descriptor $\rho(S)$ where ADR is short for "asymmetries in the distribution of roughness". This descriptor was defined in 1998 as the ratio of the squared distance between two different shape centroids (namely of area and frontier) to the squared shape diameter. After known for more than ten years, the behaviour of $\rho(S)$ was not well understood till today, thus hindering its application. Two very basic questions remained unanswered so far:

– What is the range for $\rho(S)$, if S is any bounded compact shape?

– How do shapes look like having a large $\rho(S)$ value?

This paper answers both questions. We show that $\rho(S)$ ranges over the interval $[0, 1)$. We show that the established upper bound 1 is the best possible by constructing shapes whose $\rho(S)$ values are arbitrary close to 1.

Email addresses: r.klette@auckland.ac.nz (Reinhard Klette), J.Zunic@ex.ac.uk (Joviša Žunić)

URL: www.cs.auckland.ac.nz/~rklette (Reinhard Klette), emps.exeter.ac.uk/mathematics-computer-science/staff/jz205 (Joviša Žunić)

In experiments we provide examples to indicate the kind of shapes that have relatively large $\rho(S)$ values.

Keywords: Shape, shape descriptor, shape centroid, shape diameter, image analysis, computer vision.

---

1. Introduction

Shape is an object characteristic that is most suitable for recognition, classification, or identification tasks. This is because shape allows various numerical characterizations which are particularly suitable when performing computer-based data analysis. These numerical characteristics are used as components of feature vectors allowing object comparisons, as necessary for pattern or image data analysis. It is widely accepted that comparing the objects in feature space is often more efficient than object comparison in the original object space.

A broad variety of shape descriptors has been developed so far. Some of them are very generic, such as Fourier descriptors [1], Zernike moments [15] or moment invariants [2, 6], while some other relate to specific object or shape characteristics: circularity [17, 31], convexity [18, 21, 30], rectangularity [19, 27], sigmoidality [20], orientability [32], elongation [23], tortuosity [5], and so forth. Notice that due to the diversity of shapes, we cannot expect that a particular shape descriptor would dominate others in all situations, even for a class of objects in a given application only. For this reason, different methods are developed to measure shape properties (e.g., convexity, circularity, rectangularity, and so forth).

In order to match a spectrum of specific demands for efficient object

recognition, identification or classification systems, different techniques have been used to describe the shape: algebraic invariants [6], integral invariants [14], Fourier analysis [26], statistics [16], wavelets [13], fractals [7], curvature [8, 12], integral transformations [18], computational geometry [29], and so forth.

Also note that requests vary when shape descriptors were created. A common request is that they should be invariant with respect to translation, rotation and scaling transformations, and sometimes an invariance with respect to affine transformations in general is also required. Robustness of created descriptors (e.g., required when working with low quality data) is usually ensured by considering area-based descriptors. On the other hand, high sensitivity (e.g., required when performing high-precision tasks) is usually satisfied by deciding for frontier-based descriptors. Among many other desirable properties, we just mention the tuning possibility (e.g., a possibility to control the behaviour of the descriptor by changing its parameters).

One of the properties, that is not so much studied in literature, is the geometric interpretation of designed shape descriptors. For example, the *Hu moment invariants* [6] were introduced almost 50 years ago but just recently analysed with respect to their geometric interpretation. They had been defined to satisfy invariance under similarity transforms. As such, they were used in a wide spectra of applications. But, to be able to predict (or understand) the performance to some extent (e.g. how a particular Hu descriptors will suit a certain application), it is required to have a geometric interpretation of the used descriptor. More than 45 years since the Hu moments were introduced, the authors of [25] have fully explained the geometric meaning

of those similarity-invariant features. A further step forward is due to [31]. There, the authors considered which shapes maximize or minimize a particular shape feature. For example, it has been shown that the first Hu moment invariant $\mu_{2,0}(S) + \mu_{0,2}(S)$ is minimized by circular discs, while relatively big values of $\mu_{2,0}(S) + \mu_{0,2}(S)$ are assigned to "linearly" structured shapes.

Basic geometric properties of shapes such as area $\mathcal{A}(S)$, perimeter $\mathcal{P}(S)$, or diameter $\mathcal{D}(S)$ have been used to define shape descriptors where the geometric interpretation often remains straightforward. The *shape factor* or *shape circularity measure*

$$\kappa(S) = \frac{4\pi \cdot \mathcal{A}(S)}{\mathcal{P}(S)^2} \tag{1}$$

follows the ancient isoperimetric inequality (see, e.g., Chapter 1 in [9]) that a circle has the maximum area among all shapes having the same perimeter. Values of $\kappa(S)$ range over the interval $(0, 1]$, and $\kappa(S) = 1$ is true if and only if S is a circular disc. $\kappa(S)$ is translation and rotational invariant since both shape area and shape perimeter are such invariants. Finally, elementary calculus shows that $\kappa(S)$ is scaling invariant as well.

In this paper we consider a shape descriptor which has been introduced in [11] and therein characterized to be a measure for *asymmetries in the distribution of roughness* (ADR). This *ADR-descriptor* $\rho(S)$ is defined as the ratio between the squared distance between the area-based shape centroid and the frontier-based centroid of a shape S, and the square of the shape diameter (i.e., the longest distance between two shape points). Even though $\rho(S)$ considers the ratio of two very basic geometric shape features, its behaviour was not well-understood so far, and two natural questions were not answered yet:

(1) *What is the range for $\rho(S)$?*

(2) *Which shapes reach relatively large values of $\rho(S)$?*

In this paper we answer both questions. We show that the best upper bound for $\rho(S)$ is 1. For doing so, we give a sequence of shapes $S(k)$ whose $\rho(S(k))$ value tends to 1 as $k \to \infty$. We also provide an informal, but intuitively clear description of shapes having large $\rho(S)$ values.

Notice that both shape centroids (i.e., of area or of frontier) are used widely in image normalization procedures. The area centroid of a shape is actually an average value of all the points belonging to the shape considered, while the frontier centroid is the average value of all the frontier points. Shape centroids are often used to define the shape's position, and they also play a significant role in the construction of other shape descriptors. E.g., a recent work [28] considers the distance between both shape centroids and shows that this distance is upper bounded by one fourth of the diameter, and that this upper bound cannot be improved. For another possibilities to use shape centroids to derive shape descriptors, see, for example [3, 4, 10].

The paper is organized as follows: Section 2 provides two theorems with proofs, the theoretical results of the paper. For discussions and experiments, see Sections 3 and 4. Section 5 concludes. An Appendix gives technical details for the proof of Theorem 2.

2. The Minimum Upper Bound

In this section we derive the main results of the manuscript. Before we start with theoretical considerations, we give formal definitions and denotations as used in this paper.

Throughout this paper we assume that a *shape* is represented by a bounded and compact planar region having a non-empty interior (i.e., a shape always has positive area contents).

For any shape S, its frontier ∂S is given in an arc-length parametrization $x = x(s)$ and $y = y(s)$, where $s \in [0, \mathcal{P}(S)]$. See Chapter 8 in [9] for a discussion of historic origins and variants of such a curve parametrization.

For a shape S, the *area-based centroid* $\mathcal{C}_{area}(S) = (\overline{x}_{area}(S), \overline{y}_{area}(S))$ is defined as

$$\begin{aligned} \mathcal{C}_{area}(S) &= (\overline{x}_{area}(S), \overline{y}_{area}(S)) \\ &= \left(\frac{\iint_S x \, \mathrm{d}x \, \mathrm{d}y}{\iint_S \mathrm{d}x \, \mathrm{d}y}, \frac{\iint_S y \, \mathrm{d}x \, \mathrm{d}y}{\iint_S \mathrm{d}x \, \mathrm{d}y} \right) \end{aligned} \tag{2}$$

and the *frontier-based centroid* $\mathcal{C}_{fron}(S) = (\overline{x}_{fron}(S), \overline{y}_{fron}(S))$ as

$$\begin{aligned} \mathcal{C}_{fron}(S) &= (\overline{x}_{fron}(S), \overline{y}_{fron}(S)) \\ &= \left(\frac{\int_{\partial S} x(s) \, \mathrm{d}s}{\int_{\partial S} \mathrm{d}s}, \frac{\int_{\partial S} y(s) \, \mathrm{d}s}{\int_{\partial S} \mathrm{d}s} \right) \end{aligned} \tag{3}$$

The Euclidean distance between points $p_1 = (x_1, y_1)$ and $p_2 = (x_2, y_2)$ is denoted by $d_2(p_1, p_2)$. The *shape diameter* $\mathcal{D}(S)$ is the maximum distance between two shape points:

$$\mathcal{D}(S) = \max_{p,q \in S} \{d_2(p, q)\} \tag{4}$$

The ADR shape descriptor is computed from two very basic shape features: the distance between the shape centroids and the shape diameter, and it has been introduced in [11]. This shape descriptor is denoted by $\rho(S)$ and designed to be able to measure asymmetries in the distribution of roughness indices. A formal definition is as follows:

$$\rho(S) = \frac{d_2(\mathcal{C}_{area}(S), \mathcal{C}_{fron}(S))^2}{\mathcal{D}(S)^2} \tag{5}$$

For its application for measurements in scanning electron microscopy, see [11], while some performances in classification tasks are considered in [28]. This shape measure $\rho(S)$ is translation, rotation, and scale-invariant. The range of $\rho(S)$ was unknown so far, and this is a problem for normalization procedures as commonly requested for classification tasks.

The minimum value of $\rho(S)$ is obviously 0, and this is reached for many shapes. For example, we have $\rho(S) = 0$ for all rotationally symmetric shapes S since area and frontier centroids coincide in this case. The next theorem shows that $\rho(S)$ is upper bounded by 1.

Theorem 1. *Let S be a shape. The diameter of S is upper-bounded by the distance between centroids $\mathcal{C}_{area}(S)$ and $\mathcal{C}_{fron}(S)$. In other words, the following estimate is true:*

$$\rho(S) \;=\; \frac{d_2(\mathcal{C}_{area}(S), \mathcal{C}_{fron}(S))^2}{\mathcal{D}(S)^2} \;<\; 1 \tag{6}$$

Proof. Let l be the straight line incident with two non-identical shape centroids $\mathcal{C}_{area}(S)$ and $\mathcal{C}_{fron}(S)$, and let l_{area} and l_{fron} be the lines orthogonal to l which pass through $\mathcal{C}_{area}(S)$ and $\mathcal{C}_{fron}(S)$, respectively. See Figure 1 for an example. We derive the required $d_2(\mathcal{C}_{area}(S), \mathcal{C}_{fron}(S)) < \mathcal{D}(S)$ from the fact that each line passing through $\mathcal{C}_{area}(S)$ or $\mathcal{C}_{fron}(S)$ must split the set S such that each of the two open half planes, defined by this line, has a non-empty intersection with S. We prove this statement by contradiction.[1]

[1]The authors believe that this statement can be found elsewhere, but the proof is given here to make the paper self-contained.

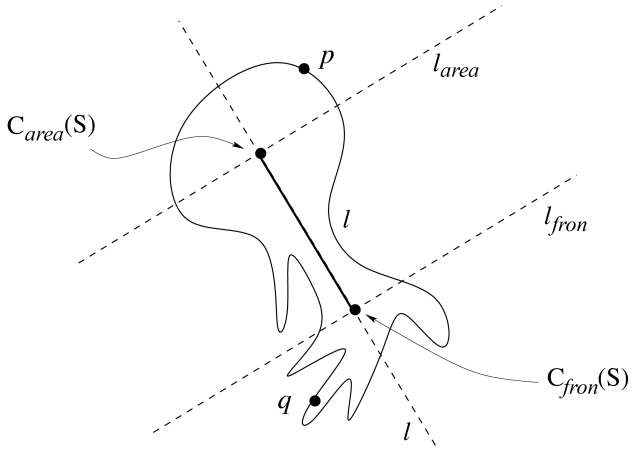

Figure 1: Straight line l is defined by the centroids of S. The straight lines l_{area} and l_{fron} are orthogonal to l, and each is incident with one of the centroids of S.

Let straight line l_{area} be given by $a \cdot x + b \cdot y + c = 0$, for some constants a, b, and c. Assume that S is contained in one of the closed half-planes defined by straight line l_{area}. Then, either $a \cdot x + b \cdot y + c \geq 0$ or $a \cdot x + b \cdot y + c \leq 0$ must be satisfied, for all $(x, y) \in S$. Let us assume that $a \cdot x + b \cdot y + c \leq 0$.

Furthermore, since S has a positive area contents, there is a subset S' of S which also has a positive area contents and whose points even satisfy the strict inequality $a \cdot x + b \cdot y + c < 0$; otherwise all the points of S would be on the line l_{area}, what is impossible because the area contents of S is greater than zero. This implies

$$\iint_{S \setminus S'} (a \cdot x + b \cdot y + c) \, \mathrm{d}x\mathrm{d}y \;\leq\; 0 \tag{7}$$

and

$$\iint_{S'} (a \cdot x + b \cdot y + c) \, \mathrm{d}x \, \mathrm{d}y \;<\; 0 \tag{8}$$

These two inequalities give the following strict inequality

$$\iint_S (a \cdot x + b \cdot y + c)\, \mathrm{d}x\, \mathrm{d}y \;=$$

$$a \cdot \iint_S x\, \mathrm{d}x\, \mathrm{d}y + b \cdot \iint_S y\, \mathrm{d}x\, \mathrm{d}y + c \cdot \iint_S \mathrm{d}x\, \mathrm{d}y < 0 \tag{9}$$

which contradicts

$$\mathcal{C}_{area}(S) = \left(\frac{\iint_S x\, \mathrm{d}x\, \mathrm{d}y}{\iint_S \mathrm{d}x\, \mathrm{d}y}, \frac{\iint_S y\, \mathrm{d}x\, \mathrm{d}y}{\iint_S \mathrm{d}x\, \mathrm{d}y} \right) \in l_{area} \tag{10}$$

Indeed, (10) is equivalent to

$$a \cdot \frac{\iint_S x\, \mathrm{d}x\, \mathrm{d}y}{\iint_S \mathrm{d}x\, \mathrm{d}y} + b \cdot \frac{\iint_S y\, \mathrm{d}x\, \mathrm{d}y}{\iint_S \mathrm{d}x\, \mathrm{d}y} + c \;=\; 0 \tag{11}$$

and obviously, Equality (11) is in contradiction to the strict Inequality (9). We have proven that S must intersect both open half-planes determined by the line l_{area}.

In an analogous way it can be shown that S intersects both open half-planes determined by the line l_{fron} by considering shape perimeter, frontier-based centroid, and line integrals instead of shape area, area-based centroid, and area integrals.

Finally, since any of the four open half-planes determined by lines l_{area} and l_{fron} contains points from S, there must be two points, say p and q, in S such that the distance $d_2(p, q)$ is larger than the distance $d_2(\mathcal{C}_{area}(S), \mathcal{C}_{fron}(S))$. □

Irrespectively of the strict Inequality (6), the upper bound provided by Theorem 1 cannot be improved, as stated by the next theorem.

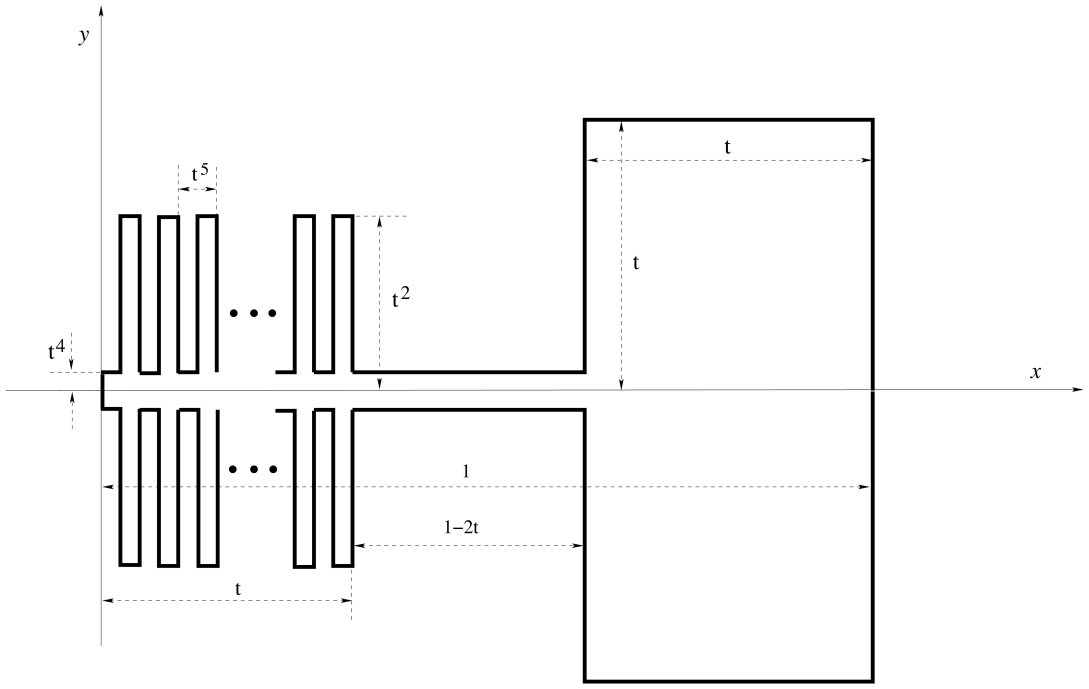

Figure 2: As $k \to \infty$, the area-based centroid $\mathcal{C}_{area}(S(k))$ converges to point $(1, 0)$, while the frontier-based centroid $\mathcal{C}_{fron}(S(k))$ goes to point $(0, 0)$. We use $t = 1/k$ for shorter notation.

Theorem 2. *For each $\varepsilon > 0$ there is a shape S such that*

$$\rho(S) \;=\; \frac{d_2(\mathcal{C}_{area}(S), \mathcal{C}_{fron}(S))^2}{\mathcal{D}(S)^2} \;>\; 1 - \varepsilon \tag{12}$$

Proof. We prove this statement by showing that there is a sequence of shapes $S(k),\ k = 1, 2, \ldots,$ with

$$\lim_{k\to\infty} \frac{d_2(\mathcal{C}_{area}(S(k)), \mathcal{C}_{fron}(S(k)))}{\mathcal{D}(S(k))} \;=\; 1 \tag{13}$$

For the definition of shapes $S(k)$, see the self-explaining Figure 2. For the sake of simplicity, we have chosen shapes symmetric about the x-axis. In

such a way we ensure that both centroids $\mathcal{C}_{area}(S(k))$ and $\mathcal{C}_{fron}(S(k))$ lie on the x-axis.

Next, let us compute the distance between the centroids of shapes $S(k)$. This is done in several intermediate steps. Calculations as given in the appendix show the following:

The area of $S(k)$ equals

$$\iint_{S(k)} \mathrm{d}x\,\mathrm{d}y \;=\; \frac{2}{k^2} + \frac{1}{k^3} + \frac{2}{k^4} - \frac{3}{k^5} \tag{14}$$

The perimeter of $S(k)$ equals

$$\int_{\partial S(k)} \mathrm{d}s \;=\; 4 \cdot k^2 + \frac{4}{k} - 2 \tag{15}$$

We use the following estimate of the x-coordinate of the area-based centroid of $S(k)$:

$$\frac{\iint_{S(k)} x\;\mathrm{d}x\,\mathrm{d}y}{\iint_{S(k)}\;\mathrm{d}x\,\mathrm{d}y} \;\geq\; \frac{\frac{2}{k^2} - \frac{1}{k^3}}{\frac{2}{k^2} + \frac{1}{k^3} + \frac{2}{k^4} - \frac{3}{k^5}} \tag{16}$$

For an estimate of the x-coordinate of the frontier-based centroid of $S(k)$, we have

$$\frac{\int_{\partial S(k)} x(s)\;\mathrm{d}s}{\int_{\partial S(k)}\;\mathrm{d}s} \;\leq\; \frac{2 \cdot k \;+\; 1 \;+\; \frac{4}{k^2} - \frac{2}{k^3}}{2 \cdot k^2 + \frac{4}{k}} \tag{17}$$

Now, from Equation (16) and from the fact that the centroid $\mathcal{C}_{area}(S(k))$ belongs to the convex hull of $S(k)$ [24], we have that

$$\frac{\iint_{S(k)} x\;\mathrm{d}x\,\mathrm{d}y}{\iint_{S(k)}\;\mathrm{d}x\,\mathrm{d}y} \in \left[\frac{\frac{2}{k^2} - \frac{1}{k^3}}{\frac{2}{k^2} + \frac{1}{k^3} + \frac{2}{k^4} - \frac{3}{k^5}}, 1\right] \tag{18}$$

which leads to

$$\lim_{k\to\infty} \frac{\iint_{S(k)} x\;\mathrm{d}x\,\mathrm{d}y}{\iint_{S(k)}\;\mathrm{d}x\,\mathrm{d}y} \;=\; 1 \tag{19}$$

Similarly, from Equation (17) and the fact that $\mathcal{C}_{fron}(S(k))$ belongs to the convex hull of $S(k)$ [24], we have that

$$\frac{\int_{\partial S(k)} x(s)\ \mathrm{d}s}{\int_{\partial S(k)}\ \mathrm{d}s} \in \left[0, \frac{2\cdot k\ +\ 1\ +\ \frac{4}{k^2} - \frac{2}{k^3}}{2\cdot k^2 + \frac{4}{k}}\right] \tag{20}$$

which leads to

$$\lim_{k\to\infty} \frac{\int_{\partial S(k)} x(s)\ \mathrm{d}s}{\int_{\partial S(k)}\ \mathrm{d}s}\ =\ 0 \tag{21}$$

Since both centroids of $S(k)$ (due to the symmetry of $S(k)$) lie on the x-axis, the last two limits give

$$\begin{aligned} &\lim_{k\to\infty} d_2(\mathcal{C}_{area}(S(k)), \mathcal{C}_{fron}(S(k))) \\ =\ & d_2((1,0),(0,0))\ =\ 1 \end{aligned} \tag{22}$$

To complete the proof it remains to show that

$$\lim_{k\to\infty} \mathcal{D}(S(k))\ =\ 1 \tag{23}$$

This is a consequence of the fact that the diameter $\mathcal{D}(S(k))$ of $S(k)$ is less than

$$\sqrt{1+\frac{4}{k^2}}$$

which equals the diameter of the minimum isothetic rectangle (i.e. with edges parallel to the coordinate axes) which encloses $S(k)$. Thus, $\mathcal{D}(S(k)) \in [1, \sqrt{1+\frac{4}{k^2}}]$ proves Equation (23). □

3. Comparison with CD-Descriptor

Both kinds of shape centroids have been utilized for defining shape descriptors before. In most cases they have been used in a shape normalisation

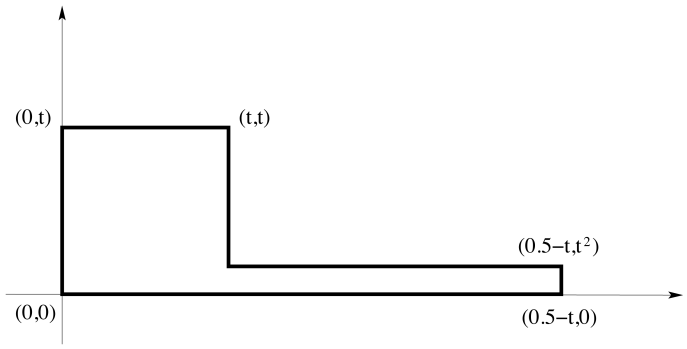

Figure 3: $P(t)$ depends on the parameter t. As $t \to 0$, the area-based centroid $\mathcal{C}_{area}(P(t))$ converges to $(0,0)$ while the frontier-based centroid $\mathcal{C}_{fron}(P(t))$ converges to $\left(\frac{1}{4},0\right)$. The perimeter of $P(t)$ converges to 1 as $t \to 0$.

phase (e.g., see [2, 6]) to provide translation invariance. But they have also been used for other purposes. A shape descriptor which is closely related to the ADR-descriptor $\rho(S)$ was introduced in [28]. The authors define a *shape centredness* descriptor $\mu(S)$, also called here *CD-descriptor*, by considering the distance between area-based and frontier-based centroids, divided by the shape perimeter $\mathcal{P}(S)$ (rather than the diameter). One result reported in [28] says that the quantity $\mu(S)$ is upper bounded by 1/4 of the shape's perimeter:

$$\mu(S) = \frac{1}{\mathcal{P}(S)} \cdot d_2(\mathcal{C}_{area}(S), \mathcal{C}_{fron}(S)) \; < \; \frac{1}{4} \tag{24}$$

The upper bound of 1/4 cannot be improved as shown in [28].

Figure 3 introduces a family of polygons $P(t)$, with $t > 0$, which satisfy

$$\lim_{t \to 0} \frac{1}{\mathcal{P}(P(t))} \cdot d_2(\mathcal{C}_{area}(P(t)), \mathcal{C}_{fron}(P(t))) = \frac{1}{4}$$

Actually, these polygons indicate that the shapes which have a unit perimeter and a relatively big distance between the centroids consist of a big "head" and a long tail.

Measures $\rho(S)$ and $\mu(S)$ are different.

Indeed, for small t values, the polygons $P(t)$ do not have any large $\rho(P(t))$ value assigned. From Figure 3 we conclude that

$$0.5 - t \leq \mathcal{D}(P(t)) \leq \sqrt{t^2 + (0.5-t)^2} \tag{25}$$

which implies that

$$\lim_{t \to 0} \mathcal{D}(P(t)) \;=\; \frac{1}{2} \tag{26}$$

Next, consider the centroids of $P(t)$ whose coordinates are computed in [28], and they are

$$\begin{aligned} \mathcal{C}_{area}(P(t)) &= \left(\frac{1}{4} \cdot \frac{5t^3 - 4t^4}{2t^2 + t^3 - 4t^4},\;\; \frac{1}{2} \cdot \frac{2t^3 + t^6 - 4t^7}{2t^2 + t^3 - 4t^4} \right) \\ \mathcal{C}_{fron}(P(t)) &= \left(\frac{1}{4} - t + 2t^2 + \frac{t^3}{2} - 2t^4,\;\; 2t^2 + \frac{t^3}{2} - t^4 \right) \end{aligned}$$

Obviously, when $t \to 0$, the area centroid $\mathcal{C}_{area}(P(t))$ approaches the origin $(0,0)$ while the frontier centroid $\mathcal{C}_{fron}(P(t))$ approaches the point $\left(\frac{1}{4}, 0\right)$. Thus, $d_2(\mathcal{C}_{area}(P(t)), \mathcal{C}_{fron}(P(t)))$ converges to $1/4$ as $t \to 0$, which, together with Equation (26), gives

$$\begin{aligned} \lim_{t \to 0} \rho(P(t)) &= \frac{d_2(\mathcal{C}_{area}(P(t)), \mathcal{C}_{fron}(P(t)))^2}{\mathcal{D}(P(t))^2} \\ &= \frac{1/16}{1/4} \;=\; \frac{1}{4} \end{aligned} \tag{27}$$

Equality (27) shows that shapes which maximize the CD-descriptor $\mu(S)$ (i.e. the distance between shape centroids with respect to their perimeter), are far away to be extreme (i.e. maximal) in the sense of the ADR-descriptor $\rho(S)$.

The opposite is true as well. Shapes $S(k)$ as considered above, which maximize the ADR-descriptor $\rho(S)$ in the limit case as $k \to \infty$, do not maximize the CD-descriptor.

More precisely, since the perimeter of the shapes $S(k)$ (see Figure 2) is equal to $4 \cdot k^2 - 2 + 4/k$ due to Equation (15), and by also using a trivial estimate $d_2\left(\mathcal{C}_{area}\left(S(k)\right), \mathcal{C}_{fron}\left(S(k)\right)\right) \leq 1$ (see Fig.2), we derive that

$$\begin{aligned} & \frac{1}{\mathcal{P}(S(k))} \cdot d_2\left(\mathcal{C}_{area}\left(S(k)\right), \mathcal{C}_{fron}\left(S(k)\right)\right) \\ \leq \; & \frac{1}{\mathcal{P}(S(k))} \; = \; \frac{1}{k^2 - 2 + 4/k} \end{aligned} \tag{28}$$

Thus, in the limit case as $k \to \infty$, the distance between centroids of the shapes $S(k)$ divided by the perimeter of $S(k)$ tends to 0, which is the theoretical minimum and far away from $1/4$ which is the best upper bound for CD-measure $\mu(S)$. We summarize:

Corollary 1. *There are shapes which maximize the CD-descriptor (e.g. minimise $\mu(S)$ values), but only define a ρ-value that is one forth of the best upper bound of the ADR-descriptor. There are shapes which maximize the ADR-descriptor (e.g. maximize $\rho(S)$ value) but minimize the CD-descriptor (e.g. minimise $\mu(S)$ value).*

4. Experiments

For an experimental illustration that the ADR-descriptor and the CD-descriptor are uncorrelated shape measures we show how they lead to different rankings of shapes for selected examples. We consider the shapes

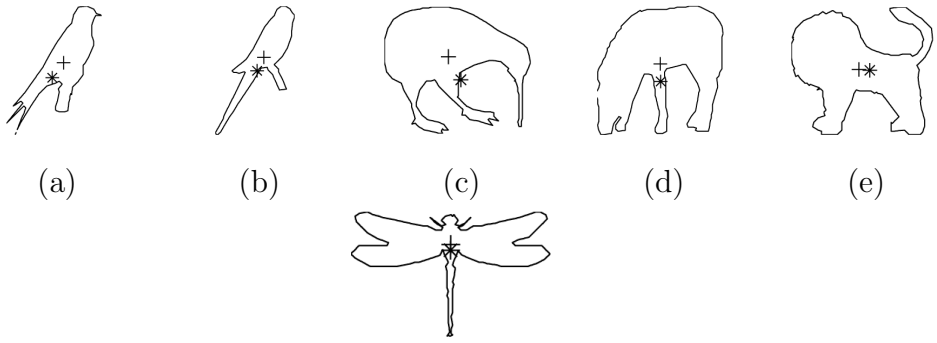

(a) (b) (c) (d) (e) (f)

Shape descriptor	(a)	(b)	(c)	(d)	(e)	(f)
$\mu(S)$	0.0407	0.0391	0.0342	0.0246	0.0153	0.0068
$\rho(S)$	0.0204	0.0126	0.0266	0.0123	0.0025	0.0010

Figure 4: Shapes are listed in accordance with their decreasing CD-descriptor values $\mu(S)$. The area-based centroids are marked with "+" while the frontier-based centroids are marked with "$*$". The table shows CD- and ADR-values for the selected shapes.

shown in Figure 4, taken from [28]. We see that the ranking according to a decreasing ADR-descriptor $\rho(S)$ equals

$$(c) - (a) - (b) - (d) - (e) - (f)$$

while the ranking according to a decreasing CD-descriptor equals

$$(a) - (b) - (c) - (d) - (e) - (f)$$

The CD-descriptor results have already been reported in [28].

With our final experiment we aim at illustrating the behaviour of the ADR-descriptor only. We apply this descriptor to shapes from the well known

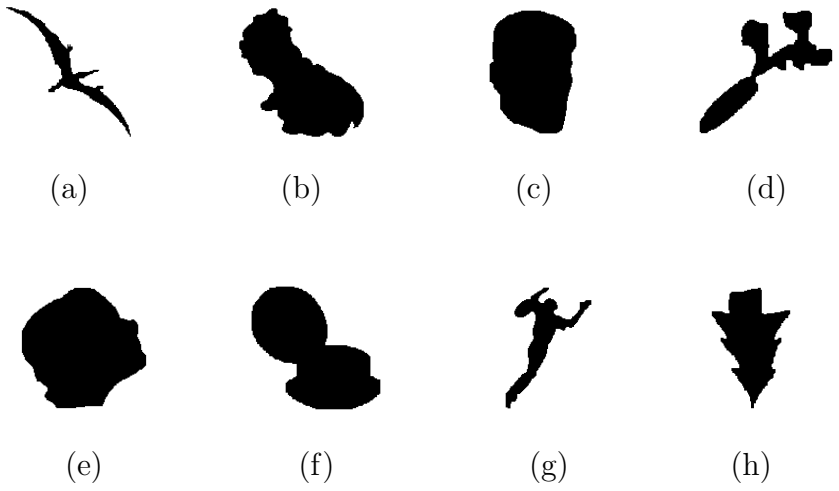

Figure 5: Shapes with small ADR-values. Actually, for all the shown cases we have that $\rho(S) = 0.0001$.

Kimia data base[2] which depicts about 22,000 different shapes.

Shapes with small $\rho(S)$ values.

First we discuss some shapes from the Kimia data base which have a very small ρ-value. Figure 5 shows shapes for which $\rho(S) = 0.0001$. Not surprising, some of those are "nearly symmetric", and we know that $\rho(S) = 0$ for all rotationally symmetric shapes. The diversity of shapes with small $\rho(S)$ values is obvious. Some of them are rather symmetric (e.g., the shape in Figure 5(h)), some are not (e.g. the shape in Figure 5(b)), some are elongated (e.g. the shape in Figure 5(a)), and some are "robust" (e.g. see Figure 5(e). These are only a few examples for the observable diversity of shapes having small ADR-values.

[2]www.lems.brown.edu/∼dmc/

Shapes with large $\rho(S)$ values.

Next, we consider shapes with relatively high $\rho(S)$-values. As proved before, there is no shape with a largest possible $\rho(S)$ value, since the lowest upper bound for $\rho(S)$ (which is 1) is never reached by any shape. This makes it more difficult to give a formal description of shapes with very large $\rho(S)$-values. However, the ADR-descriptor is not the only shape descriptor having this property. For example, the CD-descriptor from [28], the standard elongation measure (defined as the ratio of the maxima and minima of the second moment of inertia of a shape with respect to a line passing through the shape centroid; see Chapter 17 in [9]), the frontier-based elongation measure defined in [23], and others do have the same property that there is no shape defining the best upper bound.

On the other hand, a shape measure whose maximum value is reachable by some shapes usually allows us an easier description of shape which maximize measured values. Examples of such measures are the compactness measure $\kappa(S)$ (see, e.g. [17] for a definition) which is maximized by circles, or the squareness measure defined in [22] which is maximized by squares.

For large k, shapes $S(k)$ as introduced in Figure 2) are shapes having a large $\rho(S)$-value. It can be said that shape $S(k)$ consist of three geometric parts:

R-1: a "head" (on the right) whose area is $\mathcal{O}(t^2)$ and whose perimeter is $\mathcal{O}(t)$,

R-2: a "neck" (in the middle) whose area is $\mathcal{O}(t^4)$ and whose perimeter is $\mathcal{O}(1)$, and

R-3: a "tail" (on the left) whose area is $\mathcal{O}(t^3)$ and whose perimeter is $\mathcal{O}\left(\frac{1}{t^2}\right)$.

R-4: Diameters of the "head," "neck," and "tail" are $\mathcal{O}(t)$, $\mathcal{O}(1)$, and $\mathcal{O}(t)$, respectively.

Even though sets $S(k)$ are just defining one example, they indicate that "real" objects whose shape has a $\rho(S)$-value close to 1 are very rare. Indeed, as $t = \frac{1}{k}$ decreases (i.e. k tends to ∞), the relation between the orders of magnitude of area and perimeter of the "head", "neck," and "tail" are very extreme (see the asymptotic estimates in items R-1, R-2, R-3).

For example, the areas of all three parts of $S(k)$ have different orders of magnitude. The same is true for the perimeters of those parts. Also, the diameter of the "neck" is larger than the order of magnitude of the "head" or "tail"; see item R-4.

Based on the above observations, $\rho(S)$-values are not expected to be very close to 1 for real shapes because we do not expect that a real shape actually satisfies all the relations stated in R-1 to R-4. A tendency to smaller $\rho(S)$-values of real shapes is caused by the fact that $\rho(S)$ is defined as the ratio of squared values which are from the interval $[0, 1)$.

In Figure 6 we list some shapes from the Kimia data base whose $\rho(S)$ values are among the few largest values detected by us in this data base. The Kimia data base is widely used for shape studies. Because it consists of more than 22,000 shapes, it is reasonably good to represent the diversity of "real situations". Even though that such a large number of shapes was used, it turns out that none of them matches well all relations listed in items R-1 to R-4, thus coming with its ADR-value close to 1. Relatively small

$\rho(S)$-values can be expected for the shapes in the Kimia data base.

The shapes shown in Figure 6 are highly ranked with respect to their $\rho(S)$-value. Note that they also match well with most of the relations given in R-1 to R-4. Basically we notice a "good balance" between shape diameter and the distance between their shape centroids.

A relatively small diameter is caused by "multiple" tails [e.g., see Figure 6, shapes (a), (e), and (f)] or by a wrapped tail [e.g., see Figure 6 shapes (b), (c), (d), and (j)]. On the other hand, a single and stretched tail would increase the CD-value $\mu(S)$ and decrease the ADR-value $\rho(S)$. This is illustrated by shapes in Figure 7. It is worth mentioning that shapes in Figure 7 have similar characteristics as the shapes in Figure 3, that is a head with a long stretched tail.

5. Conclusion

The ADR-shape descriptor $\rho(S)$ was created in [11] to be able to characterize shapes with some degree of asymmetric distributions of roughness; the authors verified its usefulness by several experiments. However, two important questions were not answered so far, thus limiting the application of this shape descriptor: What is the range of $\rho(S)$, and how do shapes look like having a large $\rho(S)$-value? In this paper we have answered both questions.

Since there are no shapes satisfying $\rho(S) = 1$ it is not possible to say what is *the* shape which maximizes the ADR-shape descriptor. But the paper provided an informal description of shapes having a large $\rho(S)$-value. These shapes are characterized by

(i) a "head" (a part which "pulls" the area-based centroid to one side),
(ii) a "tail" which is not straight (i.e., it is crumpled or consists of several components) and which defines most of the perimeter, thus "pulling" the

(a): 0.0491 (b): 0.0510

(c): 0.0559 (d): 0.0576

(e): 0.0617 (f): 0.0639

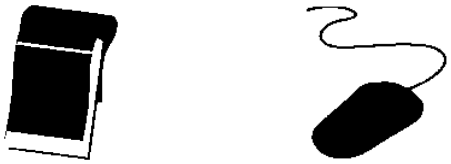

(i): 0.0866 (j): 0.0886

Figure 6: Samples of shapes from the Kimia data base having largest ADR-values $\rho(S)$ given immediately bellow each shape).

frontier-based centroid in the other side, and

(iii) a long "neck" which bridges those two parts.

Notice that apart from the descriptive characterization of shapes with a large $\rho(S)$-value, given above, a formal characterization of such shapes cannot be given. Simply, there can be many sequences of shapes, such that their corresponding $\rho(S)$-value converge to 1. For example, the rectangular "head" of the polygon S_k, in Figure 2, can be replaced by elliptical/oval ones, and the new sequence of polygons S'_k will also satisfy $\lim_{k\to\infty} \rho(S'_k) = 1$. There are many more variations in S_k which would lead to the same asymptotic, and such modifications can be done on the "tail" and "neck" part, as well.

We included several examples to illustrate how shapes look like with relatively large $\rho(S)$-values. Shapes were selected from the well-known Kimia's

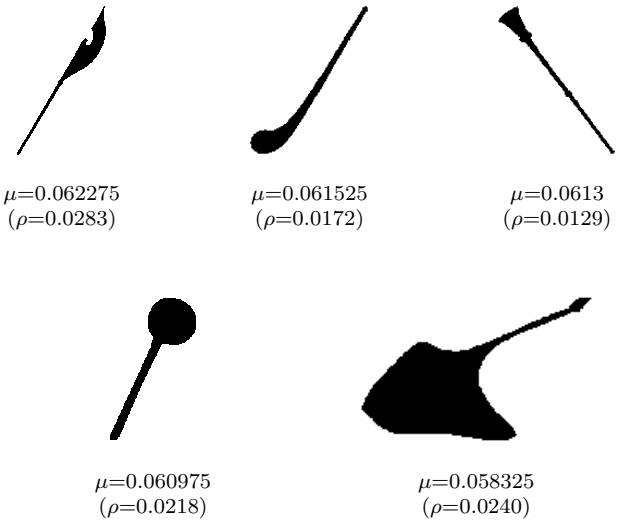

Figure 7: Samples of shapes from the Kimia database having the largest CD-values $\mu(S)$ given immediately below each shape. The $\rho(S)$-values are given in brackets for comparison.

data base consisting of around 22,000 shapes.

Similar to the ADR-descriptor, [28] defined a centredness measure, the CD-descriptor. The similarity lies in the fact that the authors of [28] also consider the distance between the shape centroids, but with respect to the shape perimeter rather than to the shape diameter. The paper showed that centredness and $\rho(S)$-values are basically uncorrelated. In conclusion we can now state that the difference between shapes having a large $\mu(S)$-value and shapes having a big $\rho(S)$-value is actually more significant than it was hypothised in [28]. Perhaps a most illustrative example for a possible big difference is the family of shapes $S(k)$ whose $\rho(S(k))$ values converge to 1 as $k \to \infty$, while $\mu(S(k))$ converges to 0 (as $k \to \infty$), and the provision of this example is also a main contribution of the paper.

It is expected that the given analysis of the ADR-descriptor will attract more interest in applying this measure in real-world shape analysis applications.

6. Acknowledgement

The authors thank Dr. Carlos Martinez-Ortiz for providing experimental results and for discussions on the presented subjects.

This work was initiated during a visit of the first author at the University of Exeter under the Royal Academy of Engineering Distinguished Visiting Fellowship Programme, and the received support is appreciated.

References

[1] E. T. Bowman, K. Soga, and T. Drummond: "Particle shape characterization using Fourier analysis," *Geotechnique,* 51:545–554, 2001.

[2] C.-C. Chen: "Improved moment invariants for shape discrimination," *Pattern Recognition,* 26:683–686, 1993.

[3] A. El-ghazal, O. Basir, and S. Belkasim: "Farthest point distance: A new shape signature for Fourier descriptors," *Signal Processing: Image Communication*, 24:572–586, 2009.

[4] I. El-Rube, N. Alajlan, M. Kamel, M. Ahmed, and G. Freeman: "MTAR: A robust 2D shape representation," *Int. J. Image and Graphics,* 6:421–443, 2006.

[5] E. Grisan, M. Foracchia, and A. Ruggeri: "A novel method for the automatic grading of retinal vessel tortuosity," *IEEE Trans. Medical Imaging,* 27:310–319, 2008.

[6] M. Hu: "Visual pattern recognition by moment invariants," *IRE Trans. Information Theory*, 8:179–187, 1962.

[7] A. R. Imre: "Dimension of time-indexed paths," *Applied Mathematics Computation,* 207:221–229, 2009.

[8] B. Kerautreta and J.-O. Lachaud: "Curvature estimation along noisy digital contours by approximate global optimization," *Pattern Recognition,* 42:2265–2278, 2009.

[9] R. Klette and A. Rosenfeld: "*Digital Geometry*," Morgan Kaufmann, San Francisco, 2004.

[10] X. Kong, Q. Luo, G. Zeng, and M. H. Lee: "A new shape descriptor based on centroid-radii model and wavelet transform," *Optics Communications,* 273:362–366, 2007.

[11] J. L. Ladaga and R. D. Bonetto: "Centroid, centroid from edge vectors, and shape descriptor using only frontier information," *J. Computer-Assisted Microscopy,* 10:1–9, 1998.

[12] H. Liu, L. J. Latecki, and W. Liu: "A unified curvature definition for regular, polygonal, and digital planar curves," *Int. J. Computer Vision*, 80:104–124, 2008.

[13] M. Maitre and M. N. Do: "Depth and color coding using shape-adaptive wavelets," *J. Visual Communication Image Representation,* 21:513–522, 2010.

[14] S. Manay, D. Cremers, B.-W. Hong, A. Yezzi, and S. Soatto: "Integral invariants for shape matching," *IEEE Trans. Pattern Analysis Machine Intelligence,* 28:1602–1618, 2006.

[15] Y. Mei and D. Androutsos: "Robust affine invariant region-based shape descriptors: The ICA Zernike moment shape descriptor and the Whitening Zernike moment shape descriptor," *IEEE Signal Processing Letters,* 16:877–880, 2009.

[16] R. A. Melter, I. Stojmenović, and J. Žunić: "A new characterization of

399 digital lines by least square fits," *Pattern Recognition Letters*, 14:83–88,
400 1993.

401 [17] D. Proffitt: "The measurement of circularity and ellipticity on a digital
402 grid," *Pattern Recognition,* 15:383–387, 1982.

403 [18] E. Rahtu, M. Salo, and J. Heikkilä: "A new convexity measure based on
404 a probabilistic interpretation of images," *IEEE Trans. Pattern Analysis*
405 *Machine Intelligence,* 28:1501–1512, 2006.

406 [19] P. L. Rosin: "Measuring shape: Ellipticity, rectangularity, and triangu-
407 larity," *Machine Vision Applications,* 14:172–184, 2003.

408 [20] P. L. Rosin: "Measuring sigmoidality," *Pattern Recognition,* 37:1735–
409 1744, 2004.

410 [21] P. L. Rosin and C. L. Mumford: "A symmetric convexity measure,"
411 *Computer Vision Image Understanding,* 103: 101–111, 2006.

412 [22] P. L. Rosin and J. Žunić: "Measuring squareness and orientation of
413 shapes," *J. Mathematical Imaging Vision,* 39:13–27, 2011.

414 [23] M. Stojmenović and J. Žunić: "Measuring elongation from shape fron-
415 tier," *J. Mathematical Imaging Vision*, 30:73–85, 2008.

416 [24] F. Valentine: "*Convex Sets*," McGraw-Hill, New York, 1964.

417 [25] D. Xu and H. Li: "Geometric moment invariants," *Pattern Recognition,*
418 41:240–249, 2008.

[26] D. Zhang and G. Lu: "A comparative study of curvature scale space and Fourier descriptors for shape-based image retrieval," *J. Visual Communication Image Representation,* 14:39–57, 2003.

[27] D. Žunić and J. Žunić: "Measuring shape rectangularity," *Electronics Letters,* 47:441–442, 2011.

[28] J. Žunić, M. A. Aktas, C. Martinez-Ortiz, and A. Galton: "The distance between shape centroids is less than a quarter of the shape perimeter," *Pattern Recognition,* 44:2161–2169, 2011.

[29] J. Žunić and P. L. Rosin: "Rectilinearity measurements for polygons," *IEEE Trans. Pattern Analysis Machine Intelligence*, 25: 1193–1200, 2003.

[30] J. Žunić and P. L. Rosin: "A new convexity measurement for polygons," *IEEE Trans. Pattern Analysis Machine Intelligence,* 26:923–934, 2004.

[31] J. Žunić, K. Hirota, and P. L. Rosin: "A Hu invariant as a shape circularity measure," *Pattern Recognition,* 43:47–57, 2010.

[32] J. Žunić, P. L. Rosin, and L. Kopanja: "On the orientability of shapes," *IEEE Trans. Image Processing*, 15:3478–3487, 2006.

Appendix: Detailed Proof of Theorem 2

We prove the statement of the theorem by showing that there is a sequence of shapes $S(k)$ such that

$$\lim_{k\to\infty} \frac{d_2(\mathcal{C}_{area}(S(k)), \mathcal{C}_{fron}(S(k)))}{\mathcal{D}(S(k))} \;=\; 1$$

Shapes $S(k)$ are described in Figure 2. For reasons of simplicity, we have chosen shapes which are symmetric about the x-axis. In such a way we guarantee that both centroids $\mathcal{C}_{area}(S(k))$ and $\mathcal{C}_{fron}(S(k))$ lie on the x-axis.

We compute the centroids of shapes $S(k)$.

- The Area of $S(k)$.

$$\iint_{S(k)} \mathrm{d}x\,\mathrm{d}y \;=\; \frac{2}{k^2} + \frac{1}{k^3} + \frac{2}{k^4} - \frac{3}{k^5}$$

Indeed, if we compute subareas of shapes $S(k)$ bounded by the vertical lines $x = 0$, $x = 1/k$, $x = 1 - 1/k$, and $x = 1$, we obtain that:

The area of the shape $S(k)$ bounded by the vertical lines $x = 0$ and $x = 1/k$ is

$$k^4 \cdot \left(\frac{2}{k^4} \cdot \frac{1}{2 \cdot k^5} + \frac{2}{k^2} \cdot \frac{1}{2 \cdot k^5} \right) = \frac{1}{k^5} + \frac{1}{k^3}$$

The area of shape $S(k)$ bounded by the vertical lines $x = 1/k$ and $x = 1 - 1/k$ is

$$\frac{2}{k^4} \cdot \left(1 - \frac{2}{k} \right) = \frac{2}{k^4} - \frac{4}{k^5}$$

The area of shape $S(k)$ bounded by the vertical lines $x = 1 - 1/k$ and $x = 1$ is

$$\frac{2}{k} \cdot \frac{1}{k} = \frac{2}{k^2}$$

- The Perimeter of $S(k)$.

  The perimeter equals

$$4 \cdot k^2 - 2 + \frac{4}{k}$$

  The total sum of horizontal edges is 2. The total sum of vertical edges is

$$4 \cdot k^4 \cdot \left(\frac{1}{k^2} - \frac{1}{k^4} \right) + \frac{4}{k} = 4 \cdot k^2 - 2 + \frac{4}{k}$$

- Estimate of the x-coordinate of the area centroid of $S(k)$.

  We show the following estimate:

$$\frac{\iint_{S(k)} x \, \mathrm{d}x \, \mathrm{d}y}{\iint_{S(k)} \mathrm{d}x \, \mathrm{d}y} \geq \frac{\frac{2}{k^2} - \frac{1}{k^3}}{\frac{2}{k^2} + \frac{1}{k^3} + \frac{2}{k^4} - \frac{3}{k^5}}$$

  The inequality follows from the estimate for the area of $S(S)$ and the following estimate:

$$\iint\limits_{S(k)} x \, \mathrm{d}x \, \mathrm{d}y \geq \iint\limits_{\substack{S(k) \\ x \geq 1 - 1/k}} x \, \mathrm{d}x \, \mathrm{d}y = \int\limits_{x=1-\frac{1}{k}}^{1} \int\limits_{y=\frac{-1}{k}}^{1/k} x \, \mathrm{d}x \, \mathrm{d}y = \frac{2}{k^2} - \frac{1}{k^3}.$$

- Estimate of the x-coordinate of the frontier-centroid of $S(k)$.

  We show the following estimate:

$$\frac{\int_{\partial S(k)} x(s) ds}{\int_{\partial S(k)} ds} \leq \frac{2 \cdot k \ + \ 1 \ + \ \frac{4}{k^2} - \frac{2}{k^3}}{2 \cdot k^2 + \frac{4}{k}}$$

  This estimate follows from the expression of the perimeter of $S(k)$ and from the following derivation.

  We split the frontier $\partial S(k)$ of $S(k)$ into the part $\partial S^h(k)$ that consists of horizontal edges, and part $\partial S^v(k)$ that consists of vertical edges. We obtain

$$\int_{\partial S(k)} x(s)\ \mathrm{d}s = \int_{\partial S^h(k)} x(s)\ \mathrm{d}s\ +\ \int_{\partial S^v(k)} x(s)\ \mathrm{d}s$$

$$= \ 2 \cdot \int_{x=0}^{1} x dx\ +\ \int_{\partial S^v(k)} x(s)\ \mathrm{d}s\ =\ 1 + \int_{\partial S^v(k)} x(s)\ \mathrm{d}s$$

$$= \ 1\ +\ \int\limits_{\substack{\partial S^v(k) \\ x \leq \frac{1}{k}}} x(s)\ \mathrm{d}s\ +\ \int\limits_{\substack{\partial S^v(k) \\ x = 1 - \frac{1}{k}}} x(s)\,\mathrm{d}\ +\ \int\limits_{\substack{\partial S^v(k) \\ x = 1}} x(s)\ \mathrm{d}s$$

$$< \ 1\ +\ \int\limits_{\substack{\partial S^v(k) \\ x \leq \frac{1}{k}}} x(s)\ \mathrm{d}s\ +\ \int_{t=-1/k^2}^{1/k^2} \left(1 - \frac{1}{k}\right) dt\ +\ \int_{t=-1/k^2}^{1/k^2} dt$$

$$= \ 1\ +\ \int\limits_{\substack{\partial S^v(k) \\ x \leq \frac{1}{k}}} x(s)\,\mathrm{d}\ +\ \frac{2}{k^2} \cdot \left(1 - \frac{1}{k}\right) + \frac{2}{k^2}$$

$$< \ 1\ +\ \frac{4}{k^2} - \frac{2}{k^3}\ +\ k^4 \cdot \int\limits_{\substack{\partial S^v(k) \\ x = \frac{1}{k}}} x(s)\ \mathrm{d}s$$

$$< \ 1\ +\ \frac{4}{k^2} - \frac{2}{k^3}\ +\ k^4 \cdot \int_{t=-1/k^2}^{1/k^2} \frac{1}{k}\,\mathrm{d}t$$

$$= \ 2 \cdot k\ +\ 1\ +\ \frac{4}{k^2} - \frac{2}{k^3}$$

Now, also take into account that the centroid $\mathcal{C}_{area}(S(k))$ belongs to the convex hull of $S(k)$. We have that

$$\frac{\iint_{S(k)} x\ \mathrm{d}x\,\mathrm{d}y}{\iint_{S(k)}\ \mathrm{d}x\,\mathrm{d}y}\ \in\ \left[\frac{\frac{2}{k^2} - \frac{1}{k^3}}{\frac{2}{k^2} + \frac{1}{k^3} + \frac{2}{k^4} - \frac{3}{k^5}}, 1\right]$$

This leads to

$$\lim_{k\to\infty} \frac{\iint_{S(k)} x \, \mathrm{d}x \, \mathrm{d}y}{\iint_{S(k)} \mathrm{d}x \, \mathrm{d}y} \;=\; 1$$

Similarly, from the fact that the centroid $\mathcal{C}_{fron}(S(k))$ belongs to the convex hull of $S(k)$ we have

$$\frac{\int_{\partial S(k)} x(s) ds}{\int_{\partial S(k)} ds} \in \left[0, \frac{2 \cdot k \;+\; 1 \;+\; \frac{4}{k^2} - \frac{2}{k^3}}{2 \cdot k^2 + \frac{4}{k}}\right]$$

and thus

$$\lim_{k\to\infty} \frac{\int_{\partial S(k)} x(s) ds}{\int_{\partial S(k)} ds} \;=\; 0$$

The last two limits, (6) and (6), give

$$\lim_{k\to\infty} d_2(\mathcal{C}_{area}(S(k)), \mathcal{C}_{fron}(S(k))) \;=\; 0$$

It remains to prove that

$$\lim_{k\to\infty} \mathcal{D}(S(k)) \;=\; 1$$

But this is just a consequence of that the diameter $\mathcal{D}(S(k))$ of $S(k)$ is less than the diameter $\sqrt{1 + \frac{4}{k^2}}$ of the minimum area isothetic rectangle (i.e. with edges parallel to the coordinate axes) which encloses $S(k)$. Thus, $\mathcal{D}(S(k)) \in [1, \sqrt{1 + \frac{4}{k^2}}]$ shows the convergence towards 1. □